

# Sunlight Mediated Heterogeneous Photocatalysis of Crystal Violet Dye Using Barium Oxide Nano Powder

Nagendra Naik K.<sup>1</sup>; Ereshanaik<sup>2</sup>; Dadapeer S.<sup>3</sup>

<sup>1</sup>Dept. of Environmental Science, Govt. First Grade College, Davangere, Karnataka, India

<sup>2</sup>Dept. of Chemistry, Sir M.V. Govt. Science College, Bommankatte, Bhadravathi, Karnataka, India

<sup>3</sup>Dept. of Physics, Govt. First Grade College, Davangere, Karnataka, India

Publication Date: 2026/01/21

**Abstract:** Crystal violet belongs to basic dye group. It is a mitotic toxin and a mutagen so there is concern regarding these chemicals making deleterious effect on biota and whole environment. Various methods have been developed for the treatment of dye effluents. Heterogeneous photocatalysis is one of the prominent ways for removing the dyes from effluent due to the ability of present method to fully mineralize the pollutant into  $\text{CO}_2$ ,  $\text{H}_2\text{O}$  and mineral acids in the presence of metal oxide nano powder as catalysts. The photo catalysis is accelerated on addition of large band-gap metal oxides nano powder. In present study,  $\text{BaO}$  nanoparticles prepared using solution combustion method and used for the discoloration of crystal violet a basic dye. Synthesized nano powder was identified by using XRD, SEM, UV-Visible spectroscopy and EDAX. The average nanoparticle size was determined to be 36 nm. The experiments were conducted by adjusting factors such as catalyst dosage, pH, dye concentration and variable irradiation. The experimental results demonstrated that, the synthesized  $\text{BaO}$  nanoparticles showed a maximum degradation of 99.10%.

**Keywords:**  $\text{BaO}$ , Crystal Violet, Photocatalysis, Nanoparticles.

**How to Cite:** Nagendra Naik K.; Ereshanaik; Dadapeer S. (2026) Sunlight Mediated Heterogeneous Photocatalysis of Crystal Violet Dye Using Barium Oxide Nano Powder. *International Journal of Innovative Science and Research Technology*, 11(1), 1262-1271. <https://doi.org/10.38124/ijisrt/26jan517>

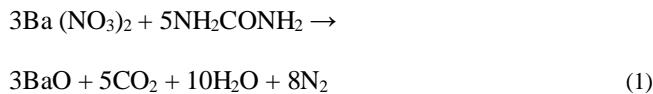
## I. INTRODUCTION

Textile industries are the major source of water pollution; the partially treated effluent containing chemicals are released to the water [1]. Around 1 million tons of dyes produced each year of which textile's dyes contribution is 50% [2]. The dyeing segment accounts for 15 to 20% of the total waste water float [3]. According to the World Bank, the fabric dyeing and finishing process contributes 17 to 20% of all industrial water pollutants. A total of 72 toxic compounds, 30 of which cannot be eliminated, have been discovered in water as a result of fabric dyeing [4]. The irrigation of textile effluent to the fields blocks the soil pores and it results in the loss of soil productivity [5]. The chemicals evaporate into the atmosphere and inhaled into the lungs and absorbed into the skin and show allergy [6]. Physical, chemical, and biological approaches are frequently used to treat effluent. Any one of these three techniques has been shown to be ineffective at removing color and other pollutants from textile wastewater. Quite 85% of undesirable chemicals can be removed using a combination of different wastewater treatment techniques [7]. In recent years, photocatalysis by semiconductors has come out as a new and highly effective technique for the elimination

of colorants and pollutants from wastewater [8]. Photocatalytic degradation of dyes has been a debated issue since the end of the 20th century [9,10]. Heterogeneous photocatalysis focuses on breaking the double and triple bonds of organic dyes into  $\text{CO}_2$ ,  $\text{H}_2\text{O}$  and mineral acids utilizing metal oxide nanoparticles as catalysts [11,12].

## II. SYNTHESIS OF METAL OXIDE NANOPARTICLES

The stoichiometric amounts of Barium nitrate,  $\text{Ba}(\text{NO}_3)_2$  (15.67g) was dissolved in a minimum quantity of water along with  $(\text{NH}_2\text{CONH}_2)$  (6g) in a silica crucible (100 cm<sup>3</sup>). The mixture was put into the muffle furnace after it had been warmed to 600 C. The solution initially boils and proceeds through dehydration, then decomposes with the development of gases ( $\text{N}_2$  and  $\text{CO}_2$ ) [13]. It then burns, producing the residue. The gases evolved produce fine metal oxide particles in addition to assisting in the heat dissipation that prevents the product from sintering. Thus, the combustion process was finished in a short amount of time [14]. The combustion reaction for the redox mixture method of synthesizing Barium oxide can be expressed as follows:



### III. CHARACTERIZATION OF BAO NANOPARTICLES

Barium oxide has a chemical formula BaO. BaO is an incombustible white hygroscopic chemical. It is used in cathode ray tubes, crown glass, and catalysts because of its cubic structure. BaO nanoparticles have the following properties:

#### A. XRD Studies of BaO

Table 1 The Computed Values of XRD Parameters of BaO

Nano particle	D(nm)	d (Å)	a (Å)	δ (10 <sup>16</sup> lines/m <sup>2</sup> )	V (Å)3
BaO	6.0469	2.734	9.025	2.734	735.091

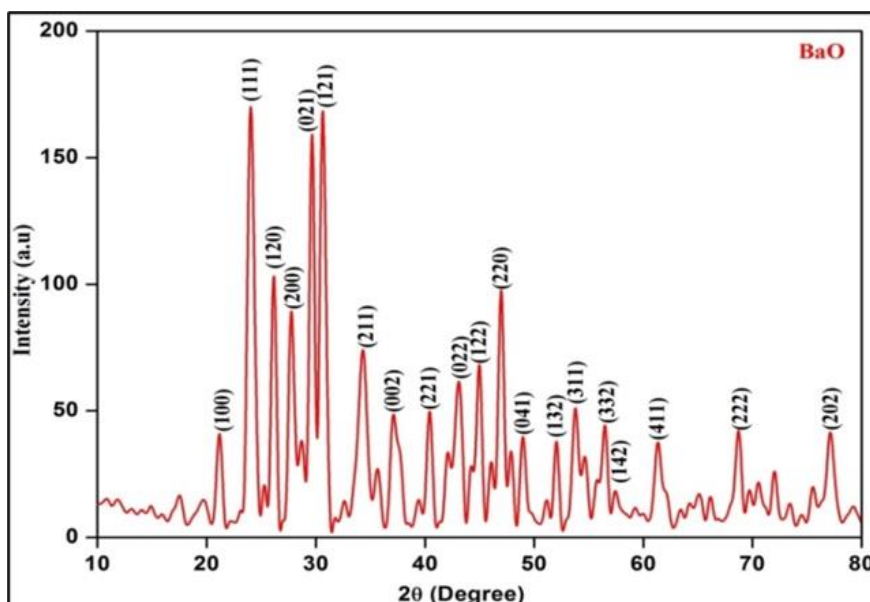


Fig. 1 XRD of Synthesized BaO Nanoparticles

Debye-Scherrer formula,

$$\text{Average crystalline size, } D = \frac{0.9 \lambda}{\beta \cos \theta} \quad (2)$$

Where,  $\lambda$ =X-ray wavelength of Cu-K $\alpha$  radiation (1.5406 Å),  $\beta$  = Full width at half maximum (in radian),  $\theta$ =Bragg's angle. Lattice parameter was analyzed by using following relation,

$$a = d_{hkl} \sqrt{h^2 + k^2 + l^2} \quad (3)$$

Where,  $d$ = Interplanar distance between two planes and  $h, k, l$ = miller indices.

$d$ - spacing values were calculated using X-ray diffraction peaks by the following relation,

$$d_{hkl} = \frac{\lambda}{2 \sin \theta} \quad (4)$$

Table 1 displays the X-Ray Diffraction patterns obtained for the Barium Oxide specimens. The peaks in this pattern are

at  $2\theta = 21.21, 23.9, 26.12, 27.7, 29.7, 30.5, 33.8$  and  $47.2$  with the hkl values  $(1\ 0\ 0), (1\ 1\ 1), (1\ 2\ 0), (2\ 0\ 0), (0\ 2\ 1), (1\ 2\ 1), (2\ 1\ 1)$  and  $(2\ 2\ 0)$  respectively. With the lattice parameters  $a=b=9.025$  and  $c=6.508$ , it is similar to the occurrence of a body-centered structure in BaO nanoparticles. The resulting values are consistent with the (JCPDS File No: 26-0178). As a result, the comparison proves that the present specimens with tetragonal crystal structures contain BaO phases. The pattern has been indexed and the lines' "d" values have been determined. XRD study of BaO nanoparticles reveals that the average crystallite size achieved was at 36nm and BaO nanoparticles size with highest peak was achieved at 6.04nm and crystallinity of 98.21%.

#### B. SEM

Scanning Electron Microscope pictures of BaO nanoparticles have revealed dispersed crystals with irregular patterns. The enlarged pictures also revealed distinct nanoparticles with sharp edges and uneven surfaces that were strongly bonded to one another [13]. (Fig. 2,3and 4).

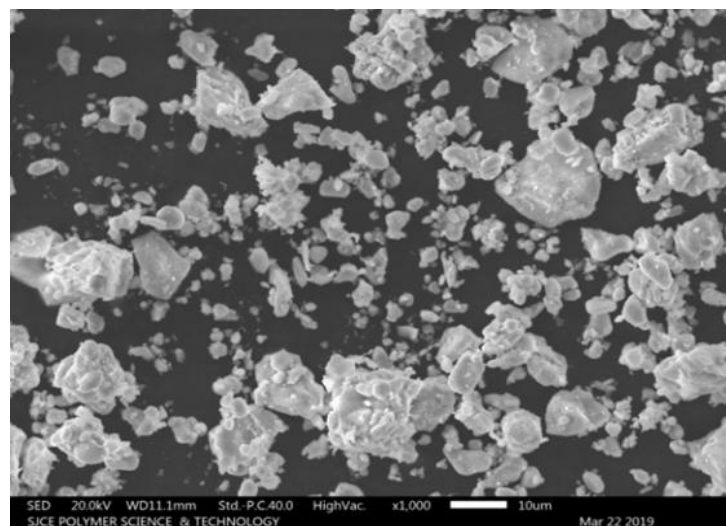


Fig. 2 Scanning Electron Micrographs of Synthesized BaO Nanoparticles

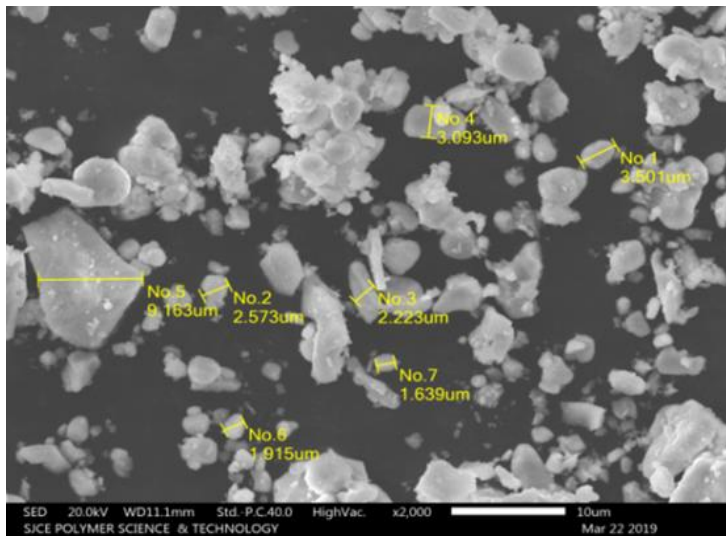


Fig. 3 Scanning Electron Micrographs of Synthesized BaO Nanoparticles

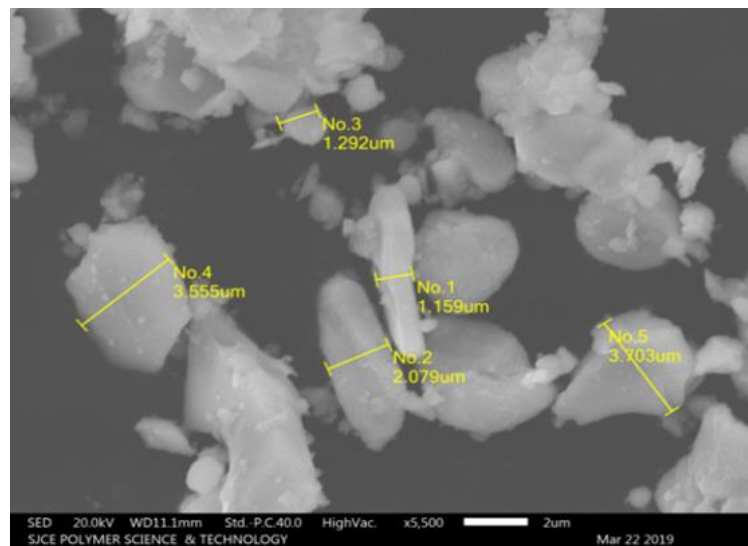


Fig. 4 Scanning Electron Micrographs of Synthesized BaO Nanoparticles

### C. UV-Vis Spectroscopy

An important tool for determining the optical band gap (OBG) of a nanomaterial is optical absorption. The elemental absorption of photons is to excite the electrons to conductivity band from the valence band. The spectrum demonstrates that the BaO nanoparticles absorb radiations more in visible region beyond 350nm [15]. The outcome of OBG is calculated using the TAUC's relation. OBG of the BaO nanoparticle is found to be 3.63eV (Fig. 5).

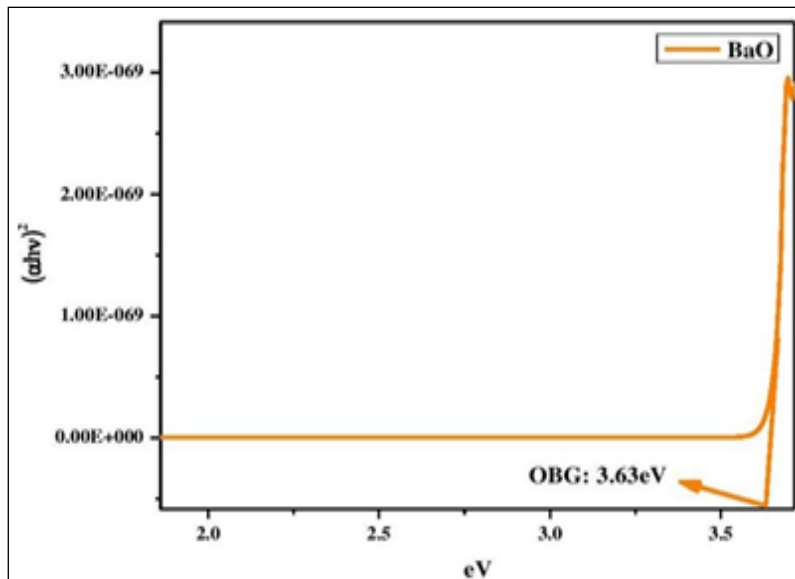


Fig. 5 UV-Absorption Spectra of Synthesized BaO Nanoparticles

### D. EDAX

The elemental analysis confirms the presence of BaO in the nanoparticle sample. Although the horizontal axis indicates energy in KeV, the number of X counts is indicated by vertical axis. (Fig. 6 and 7). The weight percentage of Carbon, Oxygen, Silicon and Barium were found to be 13.26, 20.80, 3.21, 62.73 and atomic percentage is found to be 37.11, 43.69, 3.84, and 15.35 respectively.

Table 2 Elemental Analysis of BaO

Element	Weight %	Atomic %
<b>C K</b>	13.26	37.11
<b>O K</b>	20.80	43.69
<b>Si K</b>	3.21	3.84
<b>Ba L</b>	62.73	15.35

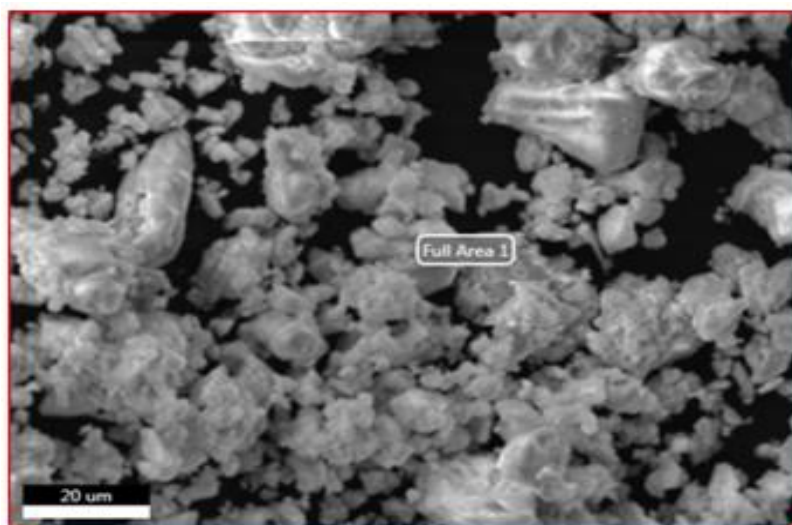


Fig. 6 SEM EDAX Image of BaO Nanoparticles

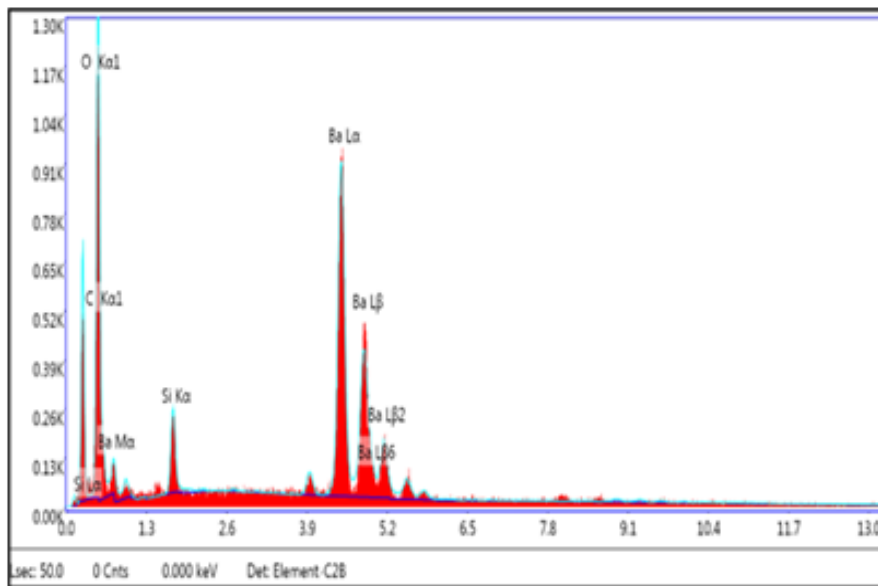


Fig. 7 EDAX of Synthesized BaO Nanoparticles

#### IV. APPLICATIONS OF BAO ON CRYSTAL VIOLET DYE

Crystal violet dye selected for the degradation experiments against BaO nanoparticles. A standard(20mg/L) crystal violet dye solution was prepared separately in 1 dm<sup>3</sup> distilled water and used for degradation study against BaO nanoparticle. Parameters such as BaO dosage, varied pH levels, dye concentrations and irradiations were employed to review the discoloration investigations, and the results were recorded. The dye solutions' pH balance was carefully maintained by adding the appropriate amounts of 1 N HCl and NaOH. Finally, using the following formula, the percentage of color degradation was determined.

$$\% \text{ Decolorization} = \frac{V_0 - V_t}{V_0} \times 100$$

$V_0$ = Initial absorbance of dye solution

$V_t$ =Absorbance at time 't'

##### A. BaO dosage

BaO dosage assorted between 0.1g to 1.0g/100ml of crystal violet dye solution. The concentration of dye solution was kept at 20ppm at pH 7 for the duration of 120 minutes. The degradation of dyes has shown the following results. Crystal violet degraded 94.05% at 0.3gm/100ml (Fig.6) in 120 minutes. Further, these dosages were kept constant for pH, dye concentrations and irradiation study.

After a repeated study optimum degradation was observed at 0.3g BaO nanopowder against crystal violet dye and at this optimum dosage, generation of OH<sup>•</sup> radicals are maximum due to optimum active sites on BaO nanoparticle. OH<sup>•</sup> radicals act as main oxidizing species for degradation of dye molecules. Further increasing the dosage level more than the optimum level will reduce the photo degradation due to the ground state catalysts being overlaid, crowded, and causing collisions [16,17].

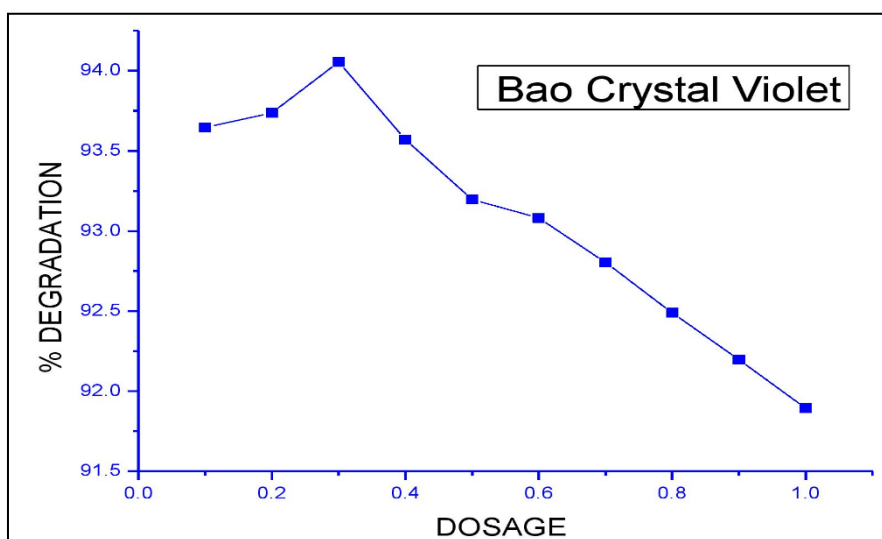


Fig. 8 Impact of BaO Concentration on Crystal Violet at 120 Minutes (Crystal violet =20 ppm, pH=7, BaO=0.3gm/100ml.)

### B. Effect of Ph

The pH range for the study was pH 2, pH 4, pH 6, pH 8, and pH 10 for dye solutions (Fig.7). The outcome indicated that, pH had a minimal influence on the degradation effectiveness. On adding BaO catalyst the degradation percentage of crystal violet dye was ranged from 99.10%, 97.94%, 97.62%, 97.13% and 96.56%, for diverse pH levels of 2, 4, 6, 8 and 10 at 120 minutes (0.3g/100ml) of BaO and Crystal violet. Maximum breakdown in this instance was at pH 2.

In present study pH parameter has shown a very minimal impact for crystal violet dye however a maximum degradation was observed in acidic condition. When the pH is acidic, photoelectrons efficiently convert  $O_2$  into  $\bullet O_2^-$  radicals and  $H_2O$  into  $OH^\bullet$  radicals [18,19]. The color degrade more quickly as a result of the production of  $OH^-$  ions and the competition between  $OH^-$  ions and crystal violet for

adsorption sites on BaO nanopowder. However, in our study, the overproduction of  $OH^\bullet$  radicals and the collision impact had an inhibitory effect on cationic dye degradation in alkaline condition [20]. At basic pH, the formation of more OH radicals have a tendency to adsorb on the catalyst's surface, which causes repulsion between like charges and leads to minimum adsorption [21]. Formation of little turbidity in the experimental samples was observed in the solutions beyond optimum pH levels [22]. These results in lesser absorption of photons by the dye solution, as a result less hydroxyl radicals were available in higher pH conditions [23]. Optimum amount of light absorbed by the dye solution in acidic condition and hence optimum  $OH^\bullet$  radicals were generated,  $OH^\bullet$  radicals in turn attack on dye molecules to disrupt the conjugated system [24]. The appearance of dye color is due to the presence of conjugated system [25]. Hence, in this study for crystal violet dye maximum degradation was observed in acidic conditions.

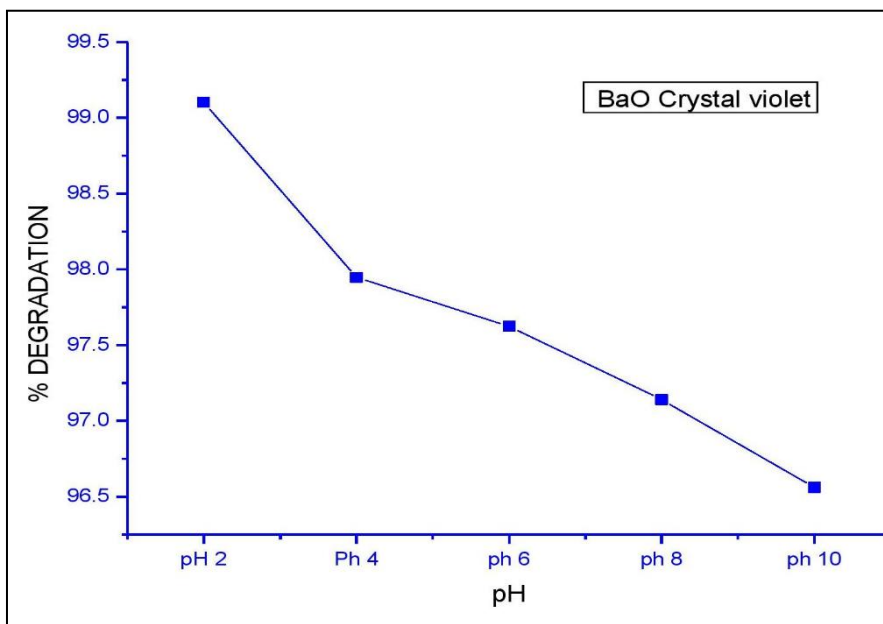


Fig. 9 (Crystal Violet = 20 ppm, BaO = 0.3 g/100 ml) Shows the Impact of pH on Crystal Violet After 120 Minutes.

### C. Dye Concentration Effects

Experiments were carried out using various concentrations of crystal violet dye from 20 ppm - 50 ppm. The degradation results for BaO against crystal violet dye are 99.10% for 20ppm, 98.43% for 30ppm 94.65% for 40ppm and 89.78% for 50ppm, respectively (Fig. 10).

During the entire experiment optimum degradation was observed at dye concentration of 20ppm. This has demonstrated that, photo degradation magnitude directly depends on the concentration of dye solution for the experimental dye. Increased dye concentration is directly proportional to reduced light penetration into the dye solution. The enhanced photo degradation is directly influenced by an elongated path length at lesser dye concentration. Pathlength reduces at higher concentrations of dye as a result less absorption of light by the catalyst [26]. This results in reduced photo degradation rate.

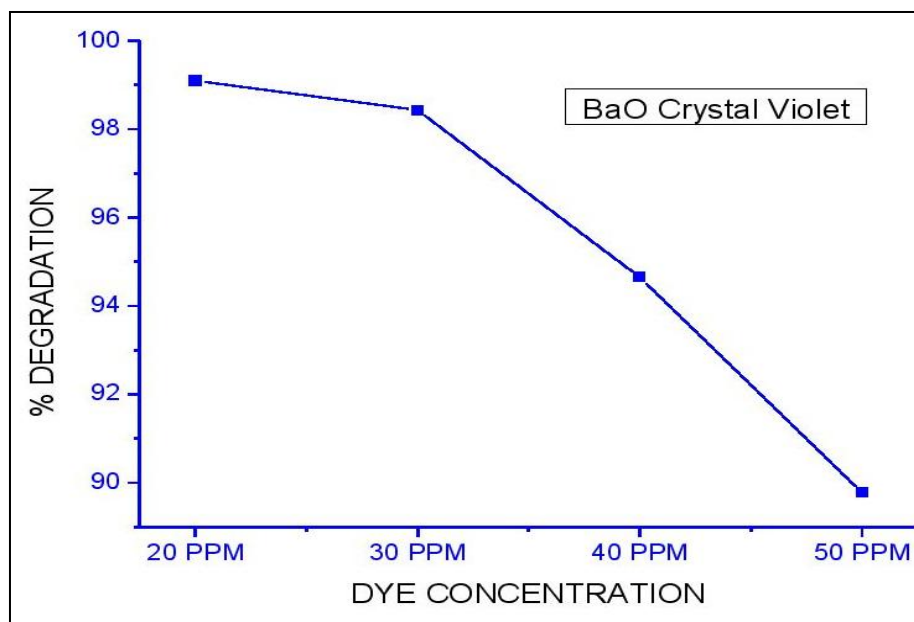


Fig. 10 Impact of Initial Dye Concentration of Crystal Violet at 120 Minutes. [BaO g/pH=0.3/2 and Crystal violet= (20, 30, 40 and 50 ppm)]

#### D. Irradiation Effect on Degradation

Irradiation experiments were conducted for the crystal violet dye. Under four varied conditions i.e., blank (crystal violet-UV/Sunlight/Dark without BaO), crystal violet-sunlight-BaO, crystal violet-UV light-BaO, crystal violet-dark-BaO experiments were carried out in order to verify the nanoparticle efficiency. For Crystal violet dye the experiments were conducted at an optimum dosage of 0.3gm/100ml, optimum pH 2 and an optimum Crystal violet concentration of 20ppm. No degradation was observed for blank (dye-sunlight/UV-light/dark without catalyst). 99.10% of discoloration was done at crystal violet-sunlight-BaO condition, 78.43% of degradation recorded at crystal violet-UV light-BaO condition and 15.00% degradation observed at dye-dark-BaO condition (Fig. 11 and 12).

This amplifies how crucial varied lighting conditions are to the mineralization of crystal violet dye. The efficient photo degradation requires both sunlight/UV light and photocatalyst. Without catalyst no degradation was observed. From this

experiment it is evident that the photon energy is absorbed primarily by the BaO catalyst to induce the primary reaction to generate OH<sup>•</sup> radicals [27]. The formation of electron hole pair on the BaO surface needs excitation of semiconductors [28]. The light supplies the excitation energy to the catalyst and hence efficient break down of organic dye molecule was succeeded [29]. In the present study, the wavelength absorbed by all the three experimental dyes was in the visible range. It is evident that, maximum absorbance of photon was recorded between (400nm – 625nm) as a result more degradation was observed in sunlight than UV light [30]. The UV light due to higher energy induces a different path of reaction and creates ions not the radicals. The resonance of energy absorbing media and energy of source should be matched. In this study visible light gives optimum energy to excite the electrons from valance band to conduction band for the creation of electron hole pair on the catalyst surface and to generate maximum OH<sup>•</sup> radicals. In addition to this the superoxide anion radicals •O<sub>2</sub><sup>-</sup> were generated more and thus plays main role under visible light irradiation to form OH<sup>•</sup> radicals [31].

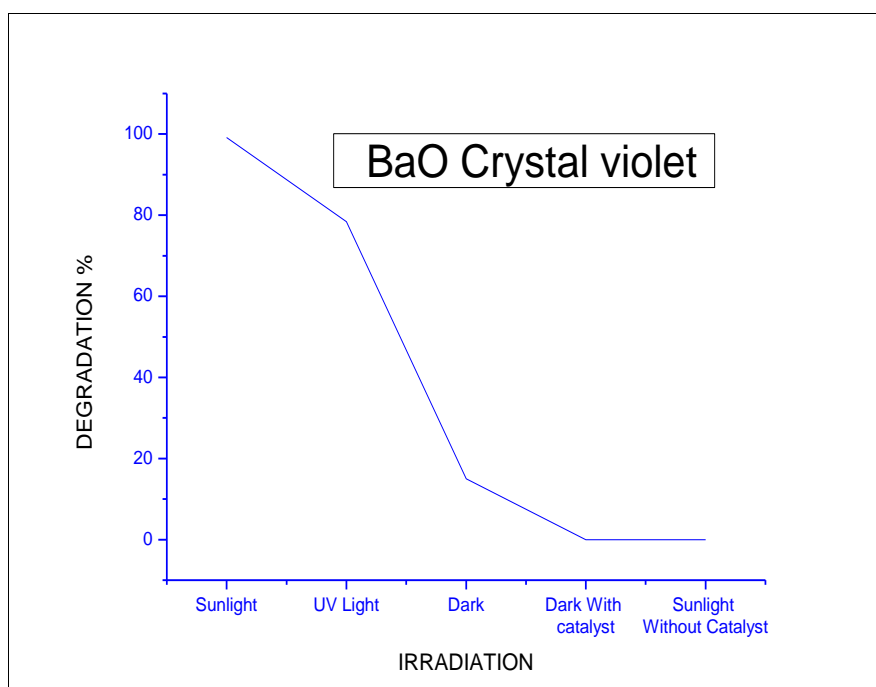


Fig. 11 shows the Impact of Sunlight Exposure on the Photocatalytic Degradation of crystal Violet Under Sunlight, Dark and UV Light Conditions for 120-Minutes.

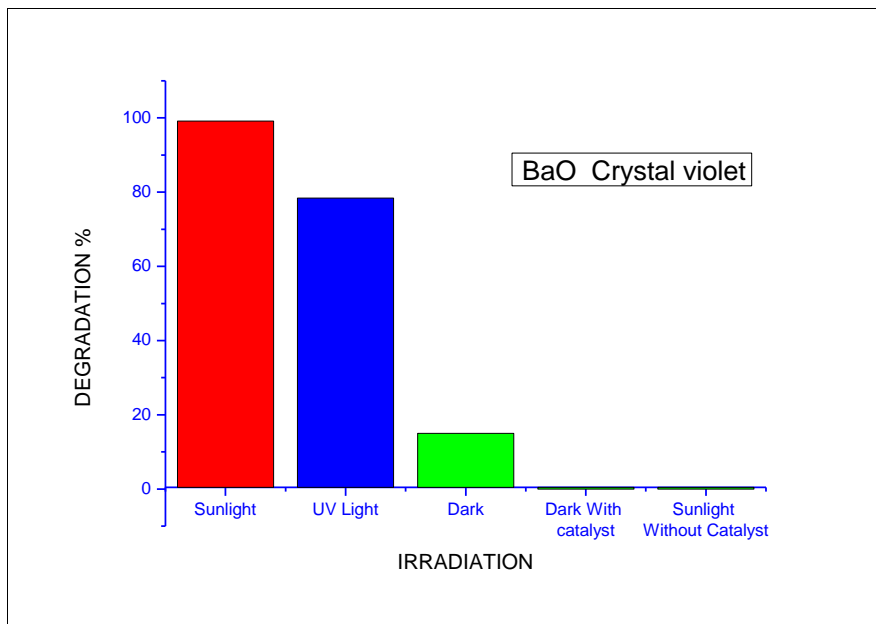


Fig. 12 Shows the Impact of Sunlight Exposure on the Photocatalytic Degradation of Crystal Violet Under Sunlight, Dark and UV Light Conditions for 120-Minutes.(b)

## V. CONCLUSION

The efficient photo degradation requires both sunlight/UV light and photocatalyst. Without catalyst no degradation was observed. 99.10% of maximum degradation achieved at dye-sunlight-BaO condition, 78.43% of degradation recorded at dye-UV light-BaO condition and 15.00% degradation observed at dye-dark-BaO condition at an optimum dye concentration of 20ppm and pH 2.

## ACKNOWLEDGMENT

The authors would like to uphold their sincere thanks to the Department of Environmental Science, Kuvempu University and Department of Collegiate Education, Karnataka.

## REFERENCES

- [1]. T. Adane, A.T. Adugna, and E. Alemayehu, "Textile industry effluent treatment techniques," *Journal of Chemistry*, vol. 2021(1), pp.5314404, 2021.
- [2]. J. Singh, N.S. Mishra, S. Banerjee, Y.C. Sharma, "Comparative studies of physical characteristics of raw and modified sawdust for their use as adsorbents for removal of acid dye," *bioresources*, vol. 6(3), pp.1, Augst 2011.
- [3]. Z. Wang, M. Xue, K. Huang, Z. Liu, "Textile dyeing wastewater treatment. Advances in treating textile effluent. Vv.5 pp. 91-116, Oct 2011.
- [4]. M. Berradi, R. Hsissou, M. Khudhair, M. Assouag, O. Cherkaoui, A. El Bachiri, A. El Harfi, "Textile finishing dyes and their impact on aquatic environs," *Heliyon*. Vol. 5(11), Nov 2019.
- [5]. D. Mohan, S.P. Shukla, "Hazardous consequences of textile mill effluents on soil and their remediation approaches," *Cleaner Engineering and Technology*. Vo. 7, pp. 100434, Apr 2022.
- [6]. W.G. Cope, "Exposure classes, toxicants in air, water, soil, domestic and occupational settings," A textbook of modern toxicology. pp. 31-48, Jan 2004.
- [7]. M.O. Awaleh, Y.D. Soubaneh, "Waste water treatment in chemical industries: the concept and current technologies," *hydrol current res.* Vol. 5, pp. 1-2, Feb 2014.
- [8]. O.K. Nayna, S.M. Tareq, "Application of semiconductor nanoparticles for removal of organic pollutants or dyes from wastewater. InNanotechnology in water and wastewater treatment," Elsevier. vol. 1, pp. 267-290, Jan 2019.
- [9]. M.K. Nazri, N. Sapawe, "A short review on photocatalytic toward dye degradation," *Materials Today: Proceedings*. vol. 1, pp. A42-47, Jan 2020.
- [10]. F. Sordello, P. Calza, C. Minero, S. Malato, M. Minella, "More than one century of history for photocatalysis, from past, present and future perspectives," *Catalysts*.vol. 12, pp. 1572, Dec 2022.
- [11]. S. Mohd, A.M. Khan, "Heterogeneous photocatalysis: Recent advances and applications," *Sustainable Green Catalytic Processes*. vol. 29, pp. 141-163, Nov 2024.
- [12]. B. Senthil Rathi, L.S. Ewe, S.S. Ewe, S.S Ewe, W.K. Yew, S.K. Tiong, "Recent trends and advancement in metal oxide nanoparticles for the degradation of dyes: synthesis, mechanism, types and its application," *Nanotoxicology*. vol. 18, pp.272-298, Apr 2024.
- [13]. A.Z. Bazeera, M.I. Amrin, "Synthesis and characterization of barium oxide nanoparticles," *IOSR J. Appl. Phys.* vol. 1, pp. 76-80, 2017.
- [14]. A.S. Veríssimo, A.M. Rocha, M. Costa, "Operational, combustion, and emission characteristics of a small-scale combustor," *Energy & Fuels*. vol. 25, pp. 2469-2480, Jan 2011.
- [15]. V. Etacheri, C. Di Valentin, J. Schneider, D. Bahnemann, S.C. Pillai, "Visible-light activation of TiO<sub>2</sub> photocatalysts: Advances in theory and experiments," *Journal of Photochemistry and Photobiology C: Photochemistry Reviews*. vol. 25, pp. 1-29, Dec 2015.
- [16]. E. C. Neyts, K. Ostrikov, M. K. Sunkara, A. Bogaerts, "Plasma catalysis: synergistic effects at the nanoscale." *Chemical reviews*. vol. 115(24), pp. 13408-13446, Dec 2015.
- [17]. N. Thirugnanam, H. Song, and Y. Wu, "Photocatalytic degradation of Brilliant Green dye using CdSe quantum dots hybridized with graphene oxide under sunlight irradiation." *Chinese J. Catalysis*. Vol. 38(12), pp. 2150-2159, Dec 2017.
- [18]. R. Dhanalakshmi, M. Muneeswaran, P. R. Vanga, M. Ashok, N. V. Giridharan, "Enhanced photocatalytic activity of hydrothermally grown BiFeO<sub>3</sub> nanostructures and role of catalyst recyclability in photocatalysis based on magnetic framework." *Applied Physics A*. vol. 122(1) pp. 13, Jan 2016.
- [19]. O. Augusto, S. Miyamoto, "Oxygen radicals and related species," *Principles of free radical biomedicine*. vol. 1, pp. 19-42, 2011.
- [20]. R. Yuan, S.N. Ramjaun, Z. Wang, J. Liu, "Concentration profiles of chlorine radicals and their significances in• OH-induced dye degradation: kinetic modeling and reaction pathways," *Chemical Engineering Journal*. vol. 209, pp 38-45, Oct 2012.
- [21]. R.V. Tikekar, N. Nitin, "Effect of physical state (solid vs. liquid) of lipid core on the rate of transport of oxygen and free radicals in solid lipid nanoparticles and emulsion," *Soft matter*. vol. 7(18), pp. 8149-8157, 2011.
- [22]. J.E. Gregor, C.J. Nokes, E. Fenton, "Optimising natural organic matter removal from low turbidity waters by controlled pH adjustment of aluminium coagulation," *Water Research*. vol. 31(12), pp. 2949-58, Dec 1997.
- [23]. X. Ding, L. Gutierrez, J.P. Croue, M. Li, L. Wang, Y. Wang, "Hydroxyl and sulfate radical-based oxidation of RhB dye in UV/H<sub>2</sub>O<sub>2</sub> and UV/persulfate systems: Kinetics, mechanisms, and comparison," *Chemosphere*. vol.253, pp.126655.Aug 2020.
- [24]. N. Ertugay, F. N. Acar, "Removal of COD and color from Direct Blue 71 azo dye wastewater by Fenton's oxidation: Kinetic study." *Arab J. Chemistry*. vol.10, pp. S1158-S1163, Feb 2017.
- [25]. P.M. Beaujuge, J.R. Reynolds, "Color control in π-conjugated organic polymers for use in electrochromic devices," *Chemical reviews*. vol.110(1), pp. 268-320, Jan 2010.
- [26]. S. Chakrabarti, B.K. Dutta, "Photocatalytic degradation of model textile dyes in wastewater using ZnO as semiconductor catalyst," *Journal of hazardous materials*. vol. 112(3), pp. 269-278, Aug 2004.
- [27]. C. C. Chen, R. J. Wu, Y. Y. Tzeng, C. S. Lu, "Chemical oxidative degradation of acridine orange dye in aqueous solution by Fenton's reagent." *J. Chinese chemical society* vol.56, pp. 1147-1155, Dec 2009.
- [28]. Y. Liu, B. Wei, L. Xu, H. Gao, M. Zhang, "Generation of oxygen vacancy and OH radicals: a comparative study of Bi<sub>2</sub>WO<sub>6</sub> and Bi<sub>2</sub>WO<sub>6</sub>- x nanoplates." *Chemistry Catalytic Chemistry*. vol. 7(24), pp. 4076-4084, Dec 2015.

- [29]. W.K. Jo, R.J. Tayade, “Recent developments in photocatalytic dye degradation upon irradiation with energy-efficient light emitting diodes,” *Chinese Journal of Catalysis*. vol. 35(11), pp. 1781-92. Nov 2014.
- [30]. R.M. Matthews, S.R. McEvoy, “A comparison of 254 nm and 350 nm excitation of TiO<sub>2</sub> in simple photocatalytic reactors,” *Journal of Photochemistry and Photobiology A: Chemistry*, vol. 66(3), pp. 355-366, Jan 1992.
- [31]. Q. Wang, H. Zhou, X. Liu, T. Li, C. Jiang, W. Song, W. Chen, “Facet-dependent generation of superoxide radical anions by ZnO nanomaterials under simulated solar light,” *Environmental Science: Nano*. Vol. 5(12), pp. 2864-2875, 2018.